FoxO1 is a crucial mediator of TGF-β/TAK1 signaling and protects against osteoarthritis by maintaining articular cartilage homeostasis

Cuicui Wang[a], Jie Shen[a,1], Jun Ying[a,b,c], Ding Xiao[a], and Regis J. O'Keefe[a,1]

[a]Department of Orthopaedic Surgery, School of Medicine, Washington University in St. Louis, St. Louis, MO 63110; [b]Institute of Orthopaedics and Traumatology, The First Affiliated Hospital of Zhejiang Chinese Medical University, 310053 Hangzhou, China; and [c]Zhejiang Chinese Medical University, 310053 Hangzhou, China

Edited by Karen M. Lyons, University of California Los Angeles, Los Angeles, CA, and accepted by Editorial Board Member Brigid L. Hogan October 14, 2020 (received for review August 12, 2020)

Transforming growth factor-β (TGF-β) signaling is a critical regulator for articular cartilage tissue maintenance and chondrocyte homeostasis. Nonetheless, the regulatory networks and downstream signaling pathways that govern the chondroprotective function of TGF-β in the context of osteoarthritis (OA) are not fully defined. Recent studies reveal that mice with postnatal deletion of triple forkhead box class Os (FoxOs) (1, 3, and 4) spontaneously develop OA-like pathologies. The OA phenotype largely recapitulates that observed in mice with loss of TGF-βR2. In the present study, we investigated the role of FoxOs as downstream mediators of TGF-β signaling and define their role in articular cartilage homeostasis. Among the three FoxOs (1, 3, and 4), TGF-β signaling exclusively regulates FoxO1 in a TGF-β activated kinase 1 (TAK1)-dependent manner. Furthermore, FoxO1 was genetically ablated in mice in a tissue-specific manner in articular cartilage or overexpressed in adult cartilage immediately followed by meniscal/ligament injury (MLI). Histological and microcomputed tomography (micro-CT) analyses demonstrated that loss of FoxO1 postnatally in articular cartilage leads to OA-like pathologies, and gain of FoxO1 in adult cartilage has both preventative and therapeutic effects on surgically induced OA. Mechanistically, FoxO1 was found to maintain articular chondrocyte homeostasis through induction of anabolic and autophagy-related gene expressions. Importantly, overexpression of FoxO1 markedly rescued the OA phenotypes caused by deficiency in TGF-β signaling in chondrocytes. Our study identifies that TGF-β/TAK1-FoxO1 is a key signaling cascade in regulation of articular cartilage autophagy and homeostasis and is a potentially important therapeutic target for OA-like joint diseases.

TGFb | FoxO1 | osteoarthritis | articular chondrocyte | autophagy

Osteoarthritis (OA) is a leading cause of impaired mobility and is the single most costly condition in the Medicare population. Despite many risk factors identified, including genetic, epigenetic, mechanical, and metabolic, the pathogenic mechanism of OA remains elusive (1–3). Consequently, there is no effective disease-modifying treatment except pain relief medication and surgical joint replacement as the only option in advanced disease (4, 5).

While OA affects the entire joint, articular cartilage degeneration remains the primary factor in altering joint function. At the cellular and molecular levels, arthritic cartilage is characterized by alteration of a healthy homeostatic state toward a catabolic state (6). Previous studies have identified transforming growth factor-β (TGF-β) signaling as an essential regulator for chondrocyte homeostasis and articular cartilage maintenance. Ablation of TGF-β-related molecules, including canonical (7–9) and noncanonical signaling (10–12), leads to hypertrophic phenotypes in articular chondrocytes and to the development of spontaneous OA in murine models. Thus, identifying downstream signaling axis and targets of TGF-β that specifically regulate a chondroprotective pathway will be extremely important in developing future disease-modifying OA drugs.

Mammalian FoxO family, comprising FoxO1, FoxO3, FoxO4, and FoxO6, are evolutionarily conserved transcriptional factors exerting seminal influences on development, longevity, and aging (13, 14). FoxO1, FoxO3, and FoxO4 are ubiquitously expressed with a high degree of functional redundancy (15), while FoxO6 is largely confined to the brain (16). FoxOs are responsive to environmental stimuli and control dynamic gene expression programs involved in both physiological and pathological processes (17). Recent mouse genetic studies demonstrate dysregulation of FoxOs and contribute to age-related tissue damage and several pathologies, including diabetes, cancer, neurodegeneration, muscle atrophy, and osteoporosis (18–20).

Similarly, FoxO expressions are recently found to be decreased in articular cartilage with aging (21). Reduced expression is observed in OA in both humans and mice and postnatal triple knockout of FoxO 1, 3, and 4 (FoxO TKO) in mice leads to the development of spontaneous OA-like pathologies (22), suggesting that FoxOs play an essential role in the maintenance of articular cartilage. Importantly, overexpression of FoxOs in chondrocytes promotes cell survival and cell anabolic response against cellular stress conditions in vitro (22, 23), implicating a

Significance

Osteoarthritis (OA) is the most prevalent joint disease and has reached epidemic proportions in the United States. Currently, there are no effective therapeutic approaches to treat OA. Thus, there is an urgent need to develop mechanistically-based therapeutic strategies to treat this disease. In this study, we identified FoxO1 as a crucial mediator of the TGF-β pathway. We also showed that loss of FoxO1 in articular cartilage leads to OA-like pathologies and gain of FoxO1 in cartilage protects against surgically and loss-of-TGF-β-induced OA. Our study defines FoxO1 as a key downstream target of TGF-β signaling and the requisite role in the maintenance of postnatal articular cartilage homeostasis and implicates modulation of FoxO1 levels/activity as a potential therapeutic strategy for OA.

Author contributions: J.S. and R.J.O. designed research; C.W., J.S., J.Y., and D.X. performed research; C.W., J.S., and J.Y. analyzed data; and C.W., J.S., and R.J.O. wrote the paper.

The authors declare no competing interest.

This article is a PNAS Direct Submission. K.M.L. is a guest editor invited by the Editorial Board.

[1]To whom correspondence may be addressed. Email: okeefer@wustl.edu or shen.j@wustl.edu.

This article contains supporting information online at https://www.pnas.org/lookup/suppl/doi:10.1073/pnas.2017056117/-/DCSupplemental.

First published November 16, 2020.

potential protective effect of FoxOs against OA. However, the specific isoform(s) that is responsible for the protective effect in chondrocytes is not established. Since FoxO TKO mice largely recapitulate the OA-like phenotypes observed in mice with loss of TGF-βR2 (7), we examined the interaction of the TGF-β signaling pathway and the FoxO transcriptional factors. Here, we analyzed the regulation of FoxO signaling by TGF-β and assessed the role of FoxO1 on joint integrity maintenance using FoxO1 loss-of-function (LOF) genetic mouse models. We further investigated the in vivo protective effect of FoxO1 gain-of-function (GOF) against OA induced by meniscal/ligament injury (MLI) injury and in the context of loss of the TGF-β pathway, and the underlying molecular mechanisms and downstream targets by which TGF-β-FoxO1 maintains articular chondrocyte homeostasis.

Results

TGF-β1 Exclusively Regulates FoxO1 but Not FoxO3 or FoxO4. In order to determine the association of the TGF-β pathway and FoxOs, articular chondrocytes were isolated and treated with TGF-β1. FoxO1 messenger RNAs (mRNAs) were significantly induced by fivefold by TGF-β1 (Fig. 1*A*). Consistent with the induction of gene expression, TGF-β1 stimulated a progressive increase in the FoxO1 protein over the control with the greatest induction at 24 h (Fig. 1*B*). In contrast, FoxO3 and FoxO4 were largely unaffected at either transcriptional or translational levels. Although FoxO4 mRNA was slightly reduced following TGF-β1 treatment, the protein expression remained unchanged over time (Fig. 1 *A* and *B*). Altogether, these results show that TGF-β1 selectively induces FoxO1 but not the other FoxO isoforms.

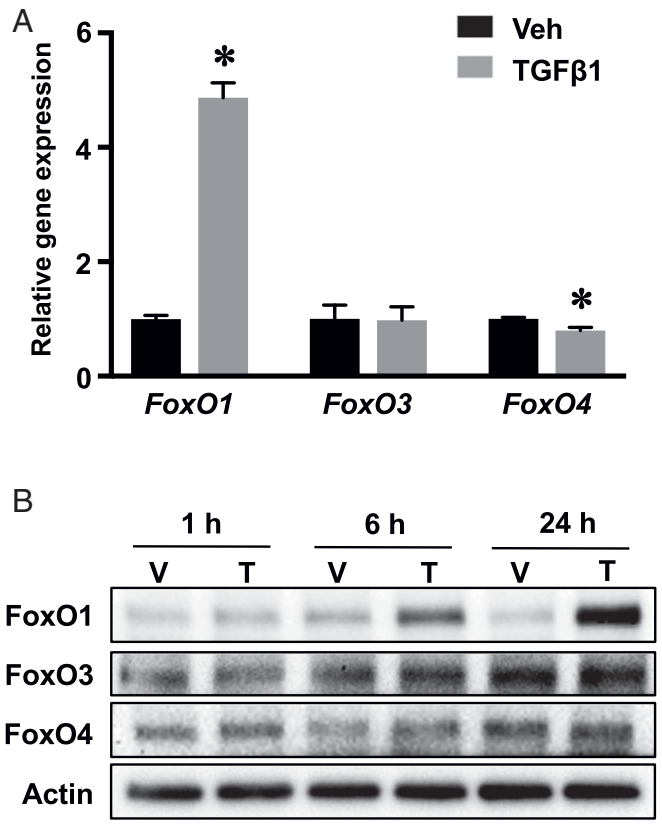

Fig. 1. TGF-β1 exclusively regulates FoxO1 but not FoxO3 or FoxO4 in a TAK1-dependent manner. (*A*) Real-time qPCR analyses for the relative expression of three FoxO isoforms in primary articular chondrocytes treated with TGF-β1 or vehicle for 24 h. The mRNA abundance was normalized to that of the gene β-actin and then normalized to the vehicle treated cells. Data are means ± SD *$P < 0.05$. $n = 3$. (*B*) Western blot analyses for protein expression in primary articular chondrocytes treated with TGF-β1 (T) or vehicle (V) for indicated times. Blots are representative of, at least, three independent experiments.

FoxO1 Deletion in Chondrocytes Leads to Catabolic Phenotype and Spontaneous OA. To determine if FoxO1 regulates the expression of key genes involved in cartilage homeostasis, FoxO1 was deleted by adenovirus-mediated transduction in *FoxO1*$^{f/f}$ articular chondrocytes. We found that FoxO1 ablation led to a significant decrease in anabolic gene expression, including *Agc1* and *Col2a1*, and increased expression of catabolic markers, including *Adamts5* and *Mmp13*, which is consistent with chondrocyte hypertrophy as reflected by a trended increase in *Col10a1* (*SI Appendix*, Fig. S1).

We, subsequently, generated FoxO1 LOF mice (*Agc1-Cre*^{ERT2}*;FoxO1*$^{f/f}$) to determine if FoxO1 is required for the maintenance of postnatal articular cartilage homeostasis. By 4 mo of age, FoxO1 LOF mice exhibited significantly thicker articular cartilage (Fig. 2 *A* and *B*). However, cellular density was markedly reduced, particularly in the noncalcified cartilage (Fig. 2*C*). Consistently, terminal deoxynucleotidyltransferase-mediated dUTP nick end labeling (TUNEL) staining revealed a significant increase in apoptotic cells in FoxO1 LOF cartilage (Fig. 2 *D* and *E*). To identify specific changes in an extracellular matrix, we performed immunohistochemistry analyses for Prg4, Col2A1, and Mmp13 on 4-mo-old cartilage. Our immunostaining demonstrated markedly reduced Prg4 and Col2A1 expression in FoxO1 LOF cartilage. We also detected substantially increased Mmp13 in the superficial zone of FoxO1 LOF cartilage, which was minimally visualized in control mice (Fig. 2*F*). In addition, picrosirius red staining, which allows for visualization of collagen fiber organization using a polarized microscope, showed abnormal collage alignment and a significant decrease in the stained area in superficial zone of FoxO1 LOF articular cartilage (*SI Appendix*, Fig. S2). These histological changes exhibited by FoxO1 LOF mice collectively suggest a shift from a homeostatic state toward a more catabolic state with altered matrix and increased cell apoptosis. By 7 mo, the FoxO1 LOF mutants (Muts) had progression to severe cartilage degeneration with some mice displaying full-thickness cartilage loss. The presence of OA was further established by an increase in the OARSI score in the FoxO1 LOF mice (Fig. 2*G*).

An additional feature of OA is a development of subchondral bone sclerosis (24). Surprisingly, micro-CT analyses revealed an overall loss of bone mass in subchondral plates of FoxO1 LOF mice as reflected by significantly reduced bone volume per total volume (BV/TV) and altered trabecular bone measures at 4 and 7 mo (*SI Appendix*, Fig. S3 and Table S1). Altogether, these data indicate a critical role of FoxO1 in maintaining articular chondrocyte homeostasis and joint integrity, and they interestingly demonstrate that the effect is unlikely due to changes in the subchondral bone.

FoxO1 Overexpression in Chondrocytes Protects against Surgically Induced OA. Because postnatal FoxO1 deletion in chondrocytes resulted in OA-like pathologies, we next determined if FoxO1 overexpression could modify disease progression in an experimental OA setting. To this end, FoxO1 GOF (*Agc1Cre*^{ERT2}*;Rosa-FoxO1*$^{f/f}$) mice were generated, and OA was introduced by MLI surgery prior to or immediately following induction of FoxO1 overexpression. In control animals, loss of proteoglycan content and cartilage surface fibrillations were observed at 8 wk following surgery and ultimately progressed to complete cartilage degeneration and synovial hyperplasia by 12 wk. In contrast, cartilage damage was attenuated, and joint integrity was better maintained in FoxO1 GOF mice at both time points (Fig. 3*A* and *SI Appendix*, Fig. S4). Moreover, FoxO1 GOF

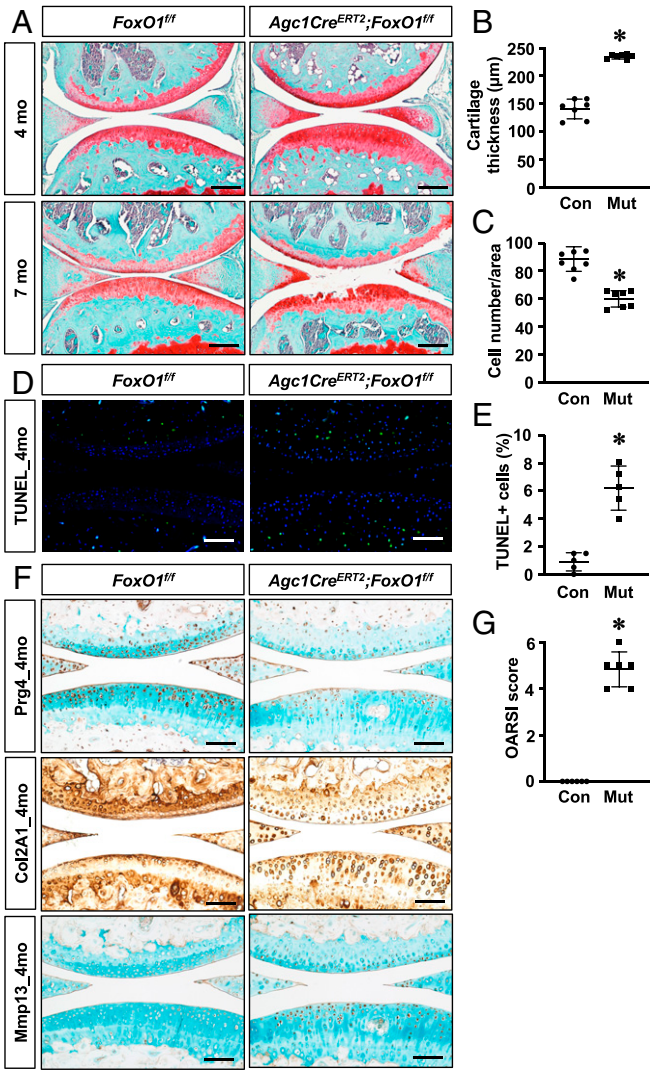

Fig. 2. FoxO1 deletion in chondrocytes leads to spontaneous OA. (*A*) Safranin O/fast green staining of knee sections of control (*FoxO1*$^{f/f}$; Ad-Con [Con]) and *FoxO1*^{Agc1ER} (Agc1Ad-Cre [Cre]^{ERT2};*FoxO1*$^{f/f}$; Mut) mice at 4 mo and 7 mo of age. All mice, including Cre negative controls, received tamoxifen. $n \geq 5$. (Scale bar, 50 μm.) (*B* and *C*) Histomorphometric analyses of cartilage thickness and chondrocyte number on knee sections at 4 mo. All results were compared to Cre negative controls and expressed as means ± SD *$P < 0.05$. $n \geq 5$. (*D* and *E*) TUNEL staining and quantification of TUNEL positive cell counts on knee sections of 4-mo-old mice. Data are means ± SD *$P < 0.05$ compared to controls. $n \geq 5$. (Scale bar, 100 μm.) (*F*) Immunohistochemical analyses for Prg4, Col2A1, and Mmp13 on knee sections of 4-mo-old mice. $n \geq 5$ (Scale bar, 100 μm.) (*G*) Osteoarthritis Research Society International (OARSI) scores for the medial tibial plateau and femoral condyle from 7-mo-old mice. *$P < 0.05$ compared to controls. $n \geq 5$.

mice exhibited better preservation of chondrocyte cellularity following MLI (Fig. 3*B*). Complementary immunohistochemistry analyses showed an increase in Prg4 in FoxO1 GOF mice at 8 wk following MLI, whereas limited staining was observed in control articular cartilage. While abundant expression of Col10A1 and Mmp13 was observed in control mice, particularly in regions with severe cartilage fibrosis and degeneration, the staining of Col10A1 and Mmp13 was substantially diminished in FoxO1 GOF cartilage, suggesting reduced hypertrophy (Fig. 3*C*). More importantly, the decrease in the severity of OA and the preservation of joint integrity by FoxO1 GOF was demonstrated by the OARSI score (Fig. 3*D*). Micro-CT analyses were also performed to determine the subchondral bone changes following MLI. Representative micro-CT images demonstrated increased subchondral bone sclerosis in the medial tibial plateau, consistent with the reactive bone formation typically found in OA. In contrast, FoxO1 GOF mice had reduced severity of bone sclerosis at 8 and 12 wk following MLI as indicated by significantly reduced BV/TV and other bone density measures (*SI Appendix*, Fig. S5 and Table S2).

Alternatively, to examine any therapeutic effect of FoxO1 on surgically induced OA, tamoxifen was administrated to *Agc1-Cre*^{ERT2};*Rosa-FoxO1*$^{f/f}$ and control mice 1 wk post-MLI surgery. Overexpression of FoxO1 after onset of OA had similar protective effects as seen in FoxO1 induction prior to MLI. Histological and micro-CT assessments revealed better preservation of cellularity and cartilage integrity, less subchondral bone sclerosis, and lower OARSI scoring in FoxO1 GOF cartilage as compared to controls at 12 wk following MLI (*SI Appendix*, Figs. S6 and S7). Together, these findings indicate that FoxO1 overexpression preserves the chondrocyte population, attenuates tissue catabolism, protects against cartilage damage, and reduces subchondral bone sclerosis in surgically induced OA.

Autophagy Is Impaired in OA Cartilage and Is Regulated by FoxO1 In Vivo. Since prior studies established that FoxOs maintain articular cartilage homeostasis through modulating autophagy, initial experiments were conducted to assess the presence of autophagy in articular chondrocytes. Our results showed that autophagy is an active process as evidenced by the robust accumulation of light chain 3 II (LC3II) from LC3I following inhibition of lysosomal function in articular chondrocytes (*SI Appendix*, Fig. S8). To assess autophagy *in vivo,* we created MLI surgery in *LC3* (green fluorescent protein -[*GFP* $^{f/+}$]) transgenic mice. Sham surgery mice had abundant GFP staining, indicating robust autophagy, particularly, in the superficial zone of articular cartilage (Fig. 4*A*). In contrast, autophagy was markedly impaired as early as 1 wk following MLI with marked reduction in GFP fluorescence. The reduced autophagy persisted through 4 wk and with the onset of phenotypical changes in cartilage. Interestingly, autophagy was markedly increased in the pseudomeniscal tissue which demonstrated an attempt at meniscus regeneration from the adjacent synovium. We next sought to determine if autophagy was altered in our genetically manipulated FoxO1 mice. Immunohistochemical staining showed reduced LC3 expression, indicating a compromised autophagy pathway in FoxO1 LOF cartilage (Fig. 4*B*). In contrast, both the joint surface and the autophagy were preserved in FoxO1 GOF mice (Fig. 4*C*). Overall, these results suggest that FoxO1 maintains chondrocyte homeostasis potentially through modulating autophagy.

TGF-β Regulates FoxO1 and Autophagy through TAK1 Signaling. We next examined the signal transduction axis through which TGF-β1 induced FoxO1 expression. TGF-β1 signals through a Smad3-dependent and a TAK1-dependent pathway. Both pathways have been shown to be active in chondrocytes (9–12). Inhibition of Smad3 activity did not alter FoxO1 protein levels by itself, nor did it affect TGF-β1-induced FoxO1 expression, even though the phosphorylation of Smad3 was suppressed as expected. Conversely, inhibition of TAK1/P38 blocked the induction of FoxO1 by TGF-β1 (Fig. 5*A*). Thus, TGF-β1 regulation of FoxO1 is TAK1 dependent but does not rely on Smad3 signaling. Of note, TGF-β1 increased both LC3I and LC3II levels, consistent with an induction of autophagy. Similarly, TAK1 appeared to be indispensable for the induction of LC3 by TGF-β1. Blockade of TAK1 signaling markedly inhibited the induction of LC3I and LC3II by TGF-β1, while blocking Smad3 signaling had no effect (Fig. 5*A*).

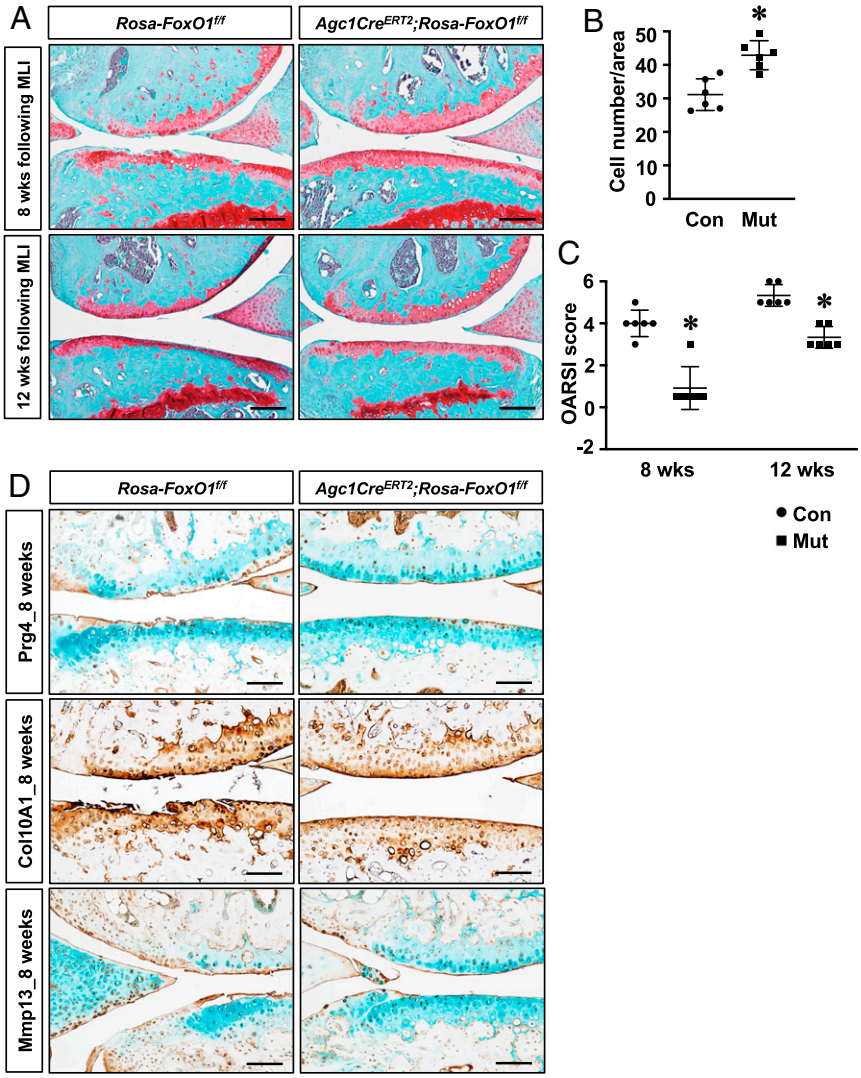

Fig. 3. Gain of FoxO1 in chondrocytes protects against surgically induced OA. (*A*) Safranin O/fast green staining of knee sections of control (*Rosa-FoxO1*$^{f/f}$; Con) and *Rosa-FoxO1*^{Agc1ER} (*Agc1Cre*^{ERT2}*;Rosa-FoxoO1*$^{f/f}$; Mut) mice at 8 and 12 wk following MLI injury. All mice, including Cre negative controls, received tamoxifen. $n \geq 5$ (Scale bar, 50 μm.) (*B*) Histomorphometric analyses of chondrocyte number on knee sections from mice at 8 wk after MLI. Data are means ± SD *$P < 0.05$ compared to controls. $n \geq 5$. (*C*) OARSI scores for the medial tibial plateau and femoral condyle at 8 and 12 wk following MLI injury. *$P < 0.05$ compared to controls. $n \geq 5$. (*D*) Immunohistochemical analyses for Prg4, Col10A1, and Mmp13 on knee sections from mice at 8 wk following MLI surgery. $n \geq 5$ (Scale bar, 100 μm.)

FoxO1 Maintains Articular Chondrocyte Homeostasis through Modulating Autophagy. The observation that TGF-β1 induces both LC3 and FoxO1 in a TAK1-dependent manner led us to investigate if the regulation of LC3/autophagy by TGF-β1 is mediated by FoxO1 in chondrocytes. We performed comprehensive in vitro experiments with virally mediated FoxO1 LOF and GOF articular chondrocytes. Our results showed that the increase in LC3I following TGF-β1 treatment was reduced as was the conversion of LC3I to LC3II upon deletion of FoxO1 (Fig. 5*B*). In contrast, FoxO1 overexpression greatly increased LC3I and LC3II protein levels (Fig. 5*C*).

We next asked whether FoxO1 is directly involved in the transcriptional regulation of autophagy-related genes. Indeed, multiple putative FoxO1 binding sites were identified in the proximal promoter of *Becn1* (25) and *Map1lc3b* (26). Binding of FoxO1 to the consensus sequences nearest the transcriptional start site in the *Becn1* and *Map1lc3b* promoters was confirmed by chromatin immunoprecipitation (ChIP) assays in ATDC5 cells (Fig. 5*D* and *SI Appendix*, Fig. S9). To determine a functional role for these promoter sequences, luciferase assays were performed in virally mediated FoxO1 GOF chondrocytes. FoxO1 overexpression led to more than 20-fold activation of the *Map1lc3b* promoter. Mut of the FoxO1 site completely abolished the induction of promoter and resulted in luciferase activity similar to that observed in the promoterless control cultures (Fig. 5*E*). These results demonstrate that FoxO1 directly targets expression of autophagy-related genes in articular chondrocytes.

Since autophagy failure results in accumulation of reactive oxygen species (ROS) and cell apoptosis (27, 28), we examined if the cellularity differences in the articular cartilage (Figs. 2*C* and 3*B*) of the FoxO1-LOF and FoxO1-GOF/MLI mice could be attributed to altered autophagy. As expected, FoxO1 LOF chondrocytes displayed higher ROS levels. Rapamycin (Rapa), a known activator of autophagy, prevented ROS accumulation in FoxO1 LOF chondrocytes with levels similar to those observed in control cells (Fig. 5 *F* and *G*). In contrast, FoxO1 overexpression effectively cleared the intracellular ROS and dramatically reduced cell apoptosis under the H_2O_2-induced stress

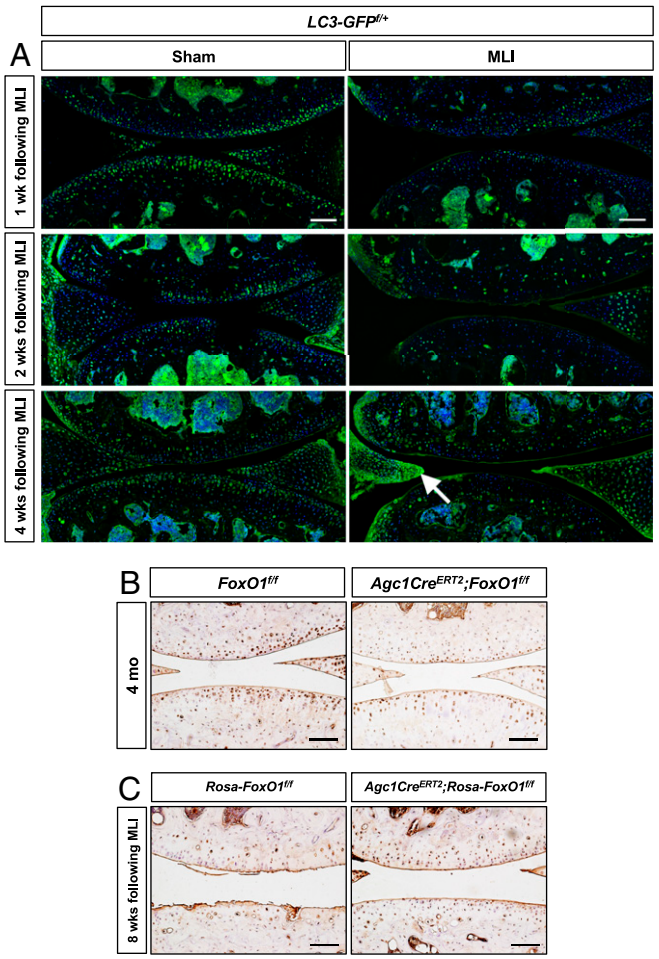

Fig. 4. LC3 is reduced following joint injury and in early OA cartilage but is maintained in articular cartilage in mice with FoxO1 GOF. (*A*) Immunofluorescence analyses for GFP on knee sections of sham or MLI-injured *LC3-GFP*$^{f/+}$ transgenic mice at indicated times. The arrow indicates the increased autophagy in the regenerated meniscal tissue. $n = 3$. (Scale bar, 100 μm.) (*B* and *C*) Immunohistochemical analyses for LC3 on knee sections of control and *FoxO1*^{Agc1ER} mice at 4 mo of age (*B*) as well as control and *Rosa-FoxO1*^{Agc1ER} mice at 8 wk following MLI surgery (*C*). $n \geq 5$. (Scale bar, 100 μm.)

condition (Fig. 5 *H–J*). Finally, we showed that the addition of Rapa to FoxO1 LOF chondrocytes shifted the cells from a catabolic state to a more homeostatic state (*SI Appendix*, Fig. S10). Altogether these findings establish that FoxO1 regulates the expression of *Maplc3b* and *Becn1*, promotes autophagy in articular chondrocytes which is essential for ROS clearance and cell survival, and protects against injury associated joint degeneration.

FoxO1 Overexpression in Chondrocytes Rescues OA Phenotypes Caused by Loss of the TGF-β Pathway. To validate the importance of the TGF-β-FoxO1 signaling axis in regulation of cartilage homeostasis and to determine if FoxO1 GOF in cartilage can protect against OA-like pathologies caused by loss of the TGF-β pathway, we generated *Col2Cre*^{ERT2}*;Tgf-βr2*$^{f/f}$*;Rosa-FoxO1*$^{f/f}$ (Tgf-βr2 LOF;FoxO1 GOF) mice in which FoxO1 was induced to overexpress in chondrocytes in context of Tgf-βr2 LOF using inducible *Col2Cre*^{ERT2} transgenic mouse line as previously reported (7).

Consistent with in vitro findings, histological and micro-CT assessments revealed that the OA phenotypes caused by deficiency in TGF-β signaling were remarkably attenuated by FoxO1 GOF in chondrocytes. Specifically, in contrast to Tgf-βr2 LOF mice exhibiting severe cartilage degeneration, thus, allowing for "bone-on-bone" contact at 3 mo, Tgf-βr2 LOF;FoxO1 GOF mice showed even thicker articular cartilage tissue with greater integrity, less aberrant subchondral bone formation, and lower OARSI scoring, reinforcing that FoxO1 is a critical downstream target of the TGF-β pathway in regulation of cartilage homeostasis (Fig. 6 *A–C* and *SI Appendix*, Fig. S11). We then performed proliferating cell nuclear antigen (PCNA) staining and found that PCNA was detected in Tgf-βr2 LOF;FoxO1 GOF cartilage, indicating that the increased cartilage tissue in Tgf-βr2 LOF;-FoxO1 GOF mice is possibly due to chondrocyte proliferation. In order to further examine the molecular alterations in Tgf-βr2 LOF;FoxO1 GOF mice, we performed immunohistochemistry analyses for Prg4, Col10A1, and Mmp13 on 3-mo-old cartilage. Our immunostaining demonstrated markedly restoration of Prg4 expression in Tgf-βr2 LOF;FoxO1 GOF cartilage, although increased expression of Col10A1 and Mmp13 was also identified Tgf-βr2 LOF;FoxO1 GOF cartilage (*SI Appendix*, Fig. S12). Notably, LC3 levels were increased in *Col2Cre*^{ERT2}*;Rosa-FoxO1*$^{f/f}$ cartilage and was greatly maintained by FoxO1 GOF despite loss of Tgf-βr2 (Fig. 6*A*), further confirming the importance of the TGF-β-FoxO1 signaling cascade in inducing autophagy-related gene expression in articular chondrocytes.

Discussion

In this study, we first demonstrated that among the three FoxOs (1, 3, and 4), TGF-β signaling solely regulates FoxO1 in a TAK1-dependent manner. Subsequently, we provided conclusive genetic evidence that loss of FoxO1 postnatally in cartilage leads to OA-like pathologies, and that overexpression of FoxO1 in adult cartilage protects against surgically and loss-of-TGF-β-induced OA. Finally, we demonstrated that TGF-β-FoxO1 signaling cascade regulates postnatal articular cartilage homeostasis through a mechanism that involves the induction of anabolic and autophagy-related gene expressions in articular chondrocytes (Fig. 7).

Since FoxO TKO mice develop OA (22) and have a phenotype similar to that observed in mice with deletion of TGF-βR2 (7), we considered a potential role of TGF-β signaling as a regulator of FoxO transcription factors in articular chondrocytes. Therefore, we sought to establish if TGF-β specifically regulates one or more of the FoxO signaling molecules and whether any of the effects of TGF-β on articular cartilage are mediated by FoxO signaling. Our data show that TGF-β1 robustly induced the FoxO1 gene and protein expression in articular chondrocytes but did not induce the other FoxO isoforms. Similarly, FoxO1 is also induced by TGF-β1 in cardiac myofibroblasts, T cells, and keratinocytes and plays a critical role in mediating the effects of TGF-β1 in the aforementioned cells (29–31). It is, thus, reasonable to speculate that FoxO1 is the essential downstream effector of TGF-β signaling in the regulation of postnatal cartilage homeostasis. Furthermore, we established that TAK1 signaling is necessary for the induction of FoxO1 by TGF-β1.

Our genetic studies established that postnatal deletion of FoxO1 in chondrocytes leads to an initial thickening of cartilage, ultimately progressing to cartilage degeneration. These findings are similar to the OA phenotypes as previously demonstrated in mice with embryonic deletion of FoxO1 and postnatal FoxO TKO (22). Although a more articular cartilage specific *Agc1Cre* transgene and a postnatal conditional gene targeting strategy were used, one concern of our study is that FoxO1 deletion was carried out in 1-mo-old mice, which are not skeletally mature. However, no significant changes were observed in the growth plate, indicating that our findings are specific to altered cellular and molecular events in articular chondrocytes but not secondary to limb growth and morphometry. In addition, the continued expression of FoxO3 and FoxO4 did not compensate for the loss

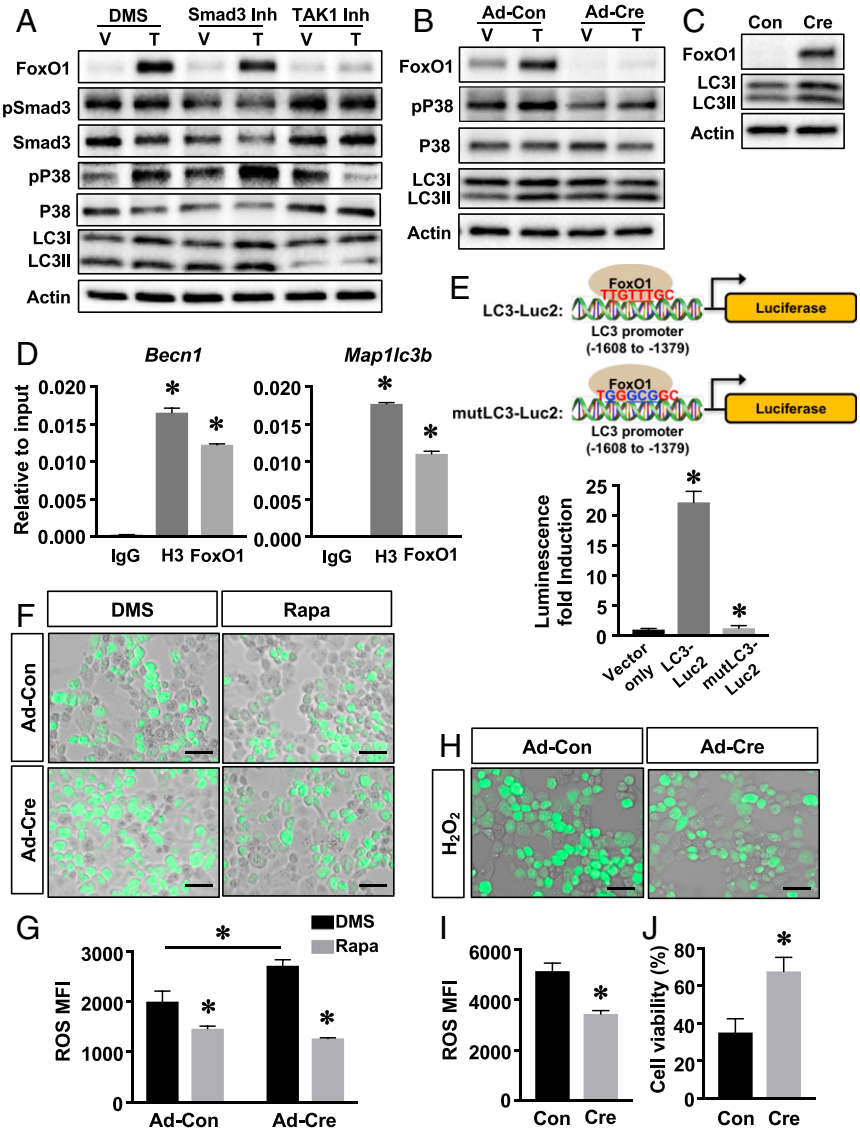

Fig. 5. FoxO1 maintains articular chondrocyte homeostasis through modulating autophagy. (*A*) Western blot analyses for protein expression in primary articular chondrocytes treated with TGF-β1 (T) or vehicle (V) in the presence of a Smad3 inhibitor (Smad3 Inh) or TAK1 inhibitor (TAK1 Inh) or dimethyl sulfoxide (DMS) for 24 h. $n = 3$. (*B*) Western blot analyses for protein expression in *FoxO1*$^{f/f}$ articular chondrocytes transduced with Con or Cre and treated with TGF-β1 (T) or vehicle (V) for 24 h. $n = 3$. (*C*) Western blot analyses for protein expression in Con or Cre transduced *Rosa-FoxO1*$^{f/f}$ articular chondrocytes. $n = 3$. (*D*) Real-time qPCR analyses for *Becn1* and *Map1lc3b* promoter regions containing the FoxO1 binding sites following pull-down of genomic DNA from ATDC5 cells with immunoglobulin G (IgG), H3 antibody, or FoxO1 antibody. Data are means ± SD *$P < 0.05$ compared to the genomic DNA immunoprecipitated by IgG. $n = 3$. (*E*) Simplified scheme for the constructs in which a luciferase reporter is driven by the LC3 promoter region containing the FoxO1 site (LC3-Luc) or mutLC3-Luc. Luciferase activity in Rosa-FoxO1f/f articular chondrocytes transduced with Cre and transfected with reporter constructs, the basic promoterless vector (Vector only), LC3-Luc2, or mutLC3-Luc2. Values are relative to those of the cells transfected with vector only and shown as means ± SD *$P < 0.05$. $n = 3$. (*F* and *G*) ROS levels was analyzed by DCF-DA staining in FoxO1f/f articular chondrocytes transduced with Con or Cre and treated with DMS or Rapa for 2 h. Mean fluorescence intensity (MFI) was calculated and shown as ± SD *$P < 0.05$ compared to DMSO treated cells or Con transduced cells. $n = 3$ (Scale bar, 50 μm.) (*H* and *I*) ROS levels in *Rosa-FoxO1*$^{f/f}$ articular chondrocytes transduced with Con or Cre and treated with H_2O_2 for 1 h. MFI was calculated and shown as ± SD *$P < 0.05$ compared to Con transduced cells. $n = 3$ (Scale bar, 50 μm.) (*J*) Cell death measured in *Rosa-FoxO1*$^{f/f}$ articular chondrocytes transduced with Con or Cre and treated with H_2O_2 for 24 h. Cell viability was calculated and shown as means ± SD *$P < 0.05$ compared to Ad-Con transduced cells. $n = 3$.

of FoxO1 and, thus, did not prevent the onset of joint degeneration. More importantly, we further provided genetic evidence using a complementary FoxO1 GOF approach in mice with MLI and confirmed FoxO1 as a disease-modifying candidate therapy for OA. FoxO1 overexpression prior to MLI injury maintained cartilage cellularity and anabolism, prevented cartilage catabolism, and inhibited MLI-associated subchondral sclerosis. Altogether, FoxO1 is clearly established as the key FoxO signaling molecule necessary for cartilage homeostasis.

Autophagy is an essential homeostatic process in tissues with a low rate of cell turnover, such as articular cartilage. Inhibition of autophagy as well as loss of autophagy with aging are associated with cell death and OA pathogenesis (32, 33). Conversely, activation of autophagy reduces the severity of experimental OA (34). Nonetheless, the pathways regulating autophagy in articular cartilage have yet to be determined. Here we provided direct evidence showing that FoxO1 transcriptionally regulates the autophagy-related genes *Becn1* and *Map1lc3b*. Consistently,

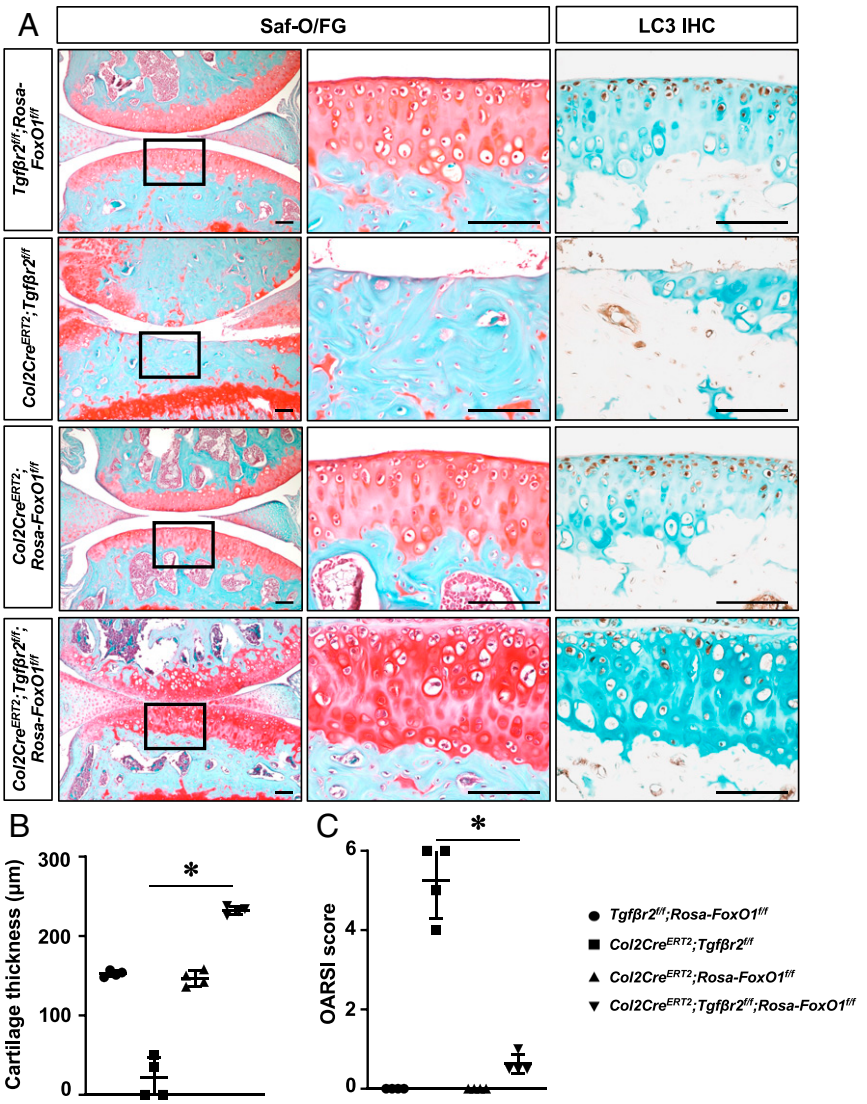

Fig. 6. FoxO1 overexpression in chondrocytes rescues OA phenotypes induced by loss of TGFβ pathway. (*A*) Safranin O/fast green staining and immunostaining for LC3 on knee sections of *Tgf-βr2$^{f/f}$;Rosa-FoxO1$^{f/f}$*, *Col2Cre^{ERT2};Tgf-βr2$^{f/f}$*, *Col2Cre^{ERT2};Rosa-FoxO1$^{f/f}$*, and *Col2Cre^{ERT2};Tgf-βr2$^{f/f}$;Rosa-FoxO1$^{f/f}$* mice at 3 mo of age. All mice, including Cre negative controls, received tamoxifen. $n = 4$ (Scale bar, 100 μm.) (*B*) Histomorphometric analyses of cartilage thickness on knee sections of *Tgf-βr2$^{f/f}$;Rosa-FoxO1$^{f/f}$*, *Col2Cre^{ERT2};Tgf-βr2$^{f/f}$*, *Col2Cre^{ERT2};Rosa-FoxO1$^{f/f}$*, and *Col2Cre^{ERT2};Tgf-βr2$^{f/f}$;Rosa-FoxO1$^{f/f}$* mice at 3 mo of age. All results were compared to *Tgf-βr2$^{f/f}$;Rosa-FoxO1$^{f/f}$* mice and expressed as means ± SD $*P < 0.05$. $n = 4$. (*C*) OARSI scores for the medial tibial plateau and femoral condyle from 3-mo-old mice. $*P < 0.05$ compared between *Col2Cre^{ERT2};Tgf-βr2$^{f/f}$*, and *Col2Cre^{ERT2};Tgf-βr2$^{f/f}$;Rosa-FoxO1$^{f/f}$* mice. $n = 4$.

FoxO1 overexpression increased LC3I and LC3II protein levels. Nonetheless, the autophagic flux evidenced by LC3II accumulation upon bafilomycin treatment was not significantly induced in articular chondrocytes with a gain of FoxO1 (*SI Appendix*, Fig. S13). Since the autophagic/lysosomal pathway is constitutively activated in normal articular cartilage (*SI Appendix*, Fig. S5 and Fig. 4*A*), it is, thus, reasonable to speculate that induction of LC3 by FoxO1 is necessary to replenish the LC3 protein pool, allowing appropriate progression of autophagy. This concept is supported by the findings that overexpression of LC3 is not sufficient to trigger autophagy in fed mice (35). Therefore, at a minimum, FoxO1 is permissive of autophagy and is necessary for normal autophagic function in cartilage. Apart from FoxO1-mediated regulation of autophagy, our results showed that conversion of LC3II from LC3I was completely blocked by TAK1 inhibition, implicating a fundamental role of TAK1 in autophagy activation in articular chondrocytes. Future studies will lead to better understanding of the complexity of the regulatory networks controlling autophagy via the TGF-β signaling pathway in the context of OA.

Autophagy failure in resting cells leads to accumulation of damaged proteins and dysfunctional organelles, especially mitochondria with generation of excess ROS that result in senescence or cell death (27, 28). Our study revealed that loss of FoxO1 resulted in enhanced intracellular ROS levels which were effectively eradicated by activation of autophagy with Rapa. Conversely, we found that FoxO1 GOF inhibited H_2O_2-induced cell apoptosis in vitro. Similarly, our results demonstrated that FoxO1 GOF preserved cellularity in vivo in the surgically induced OA, a model in which autophagy has been shown to be compromised (32). Based on these findings, along with the beneficial effect of Rapa on experimental OA as previously described (34), it is worthwhile to explore if activation of autophagy could reduce cell death, attenuate cartilage catabolism, and

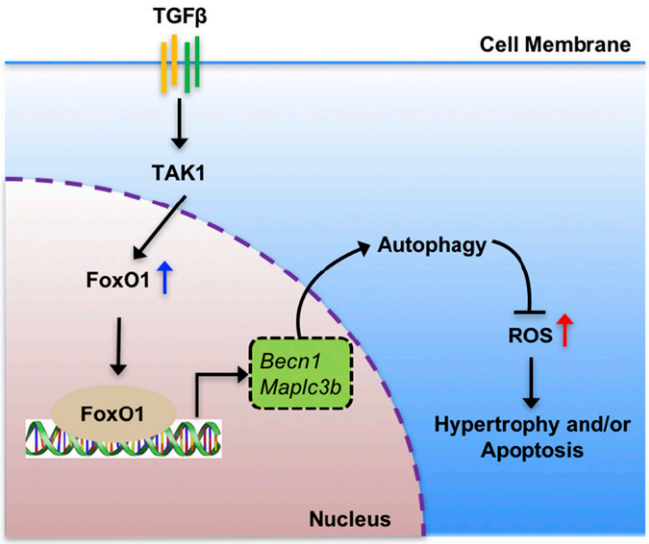

Fig. 7. Schematic model of FoxO1-mediated autophagy in articular chondrocyte homeostasis. FoxO1 is induced by TAK1-dependent TGF-β signaling. FoxO1 directly binds to gene promoter and activates autophagy-related genes, including *Becn1* and *Map1lc3b*. This transcription-dependent regulation of autophagy is crucial for the replenishment of autophagy protein pool, allowing appropriate progression of autophagy. Maintenance of autophagy in articular chondrocytes can prevent ROS accumulation and cell apoptosis.

protect against OA progression. A surprise finding of this study is that FoxO1 LOF mice displayed significant bone loss in their subchondral plates. It is well established that stress conditions, such as high levels of ROS, can trigger the translocation of FoxOs from the cytoplasm to the nucleus leading to FoxOs activation (36, 37). In fact, FoxOs activation by accumulation of age-associated cellular stressors has recently been implicated in the pathogenic mechanisms in the development of involutional osteoporosis (38). Whether this is the reason for the bone loss in the present study remains to be further determined.

While our study highlights FoxO1 is a critical downstream effector of the TGF-β/TAK1 noncanonical signaling pathway in the regulation of articular cartilage homeostasis, the precise molecular details remain to be elucidated. Our mechanistic data demonstrate FoxO1 GOF markedly ameliorates the OA phenotypes caused by loss of TGF-β signaling; however, the mechanism by which TGF-β/FoxO1 regulates articular chondrocyte proliferation and homeostasis needs more investigation. It is important to note our data do not exclude the possibility that additional downstream effectors of the TGF-β/TAK1 noncanonical pathway are required for maintenance of articular chondrocyte homeostasis. Regardless, our data identify a key signaling cascade of TGF-β/TAK1-FoxO1 in regulating articular cartilage autophagy and homeostasis. The chondroprotective effects of FoxO1 on the injury-induced OA suggest that targeting activation of FoxO1 is a novel and compelling candidate therapy for human OA. In particular, we found that TGF-β/TAK1-FoxO1-mediated autophagy is likely a key cellular participant in maintaining joint cartilage integrity.

Materials and Methods

Mice. All animal studies were performed in accordance with approval of the Committees on Animal Resources in Washington University in St. Louis. *FoxO1* floxed mice (JAX, no. 024756) (15) and *Rosa-FoxO1* floxed mice (JAX, no. 016262) (39) were previously described and were purchased from Jackson Laboratory. *Agc1Cre^{ERT2}* mice (40) and *LC3-GFP$^{f/+}$* mice (35) were generous gifts from the laboratory of Dr. Benoit de Crombrugghe (Department of Genetics, University of Texas MD Anderson Cancer Center, Houston, TX), and the laboratory of Dr. Herbert Virgin (Department of Pathology and Immunology, Washington University in St. Louis, St. Louis, MO), respectively. *FoxO1$^{f/f}$*, *Agc1Cre^{ERT2};FoxO1$^{f/f}$* (*FoxO1^{Agc1ER}*), *Rosa-FoxO1$^{f/f}$*, *Agc1Cre^{ERT2};Rosa-FoxO1$^{f/f}$* (*Rosa-FoxO1^{Agc1ER}*), *Tgf-βr2$^{f/f}$;Rosa-FoxO1$^{f/f}$*, *Col2Cre^{ERT2};Tgf-βr2$^{f/f}$*, *Col2Cre^{ERT2};Rosa-FoxO1$^{f/f}$*, *Col2Cre^{ERT2};Tgf-βr2$^{f/f}$;Rosa-FoxO1$^{f/f}$* were viable and produced in Mendelian ratios. Tamoxifen was administrated daily at a dose of 1-mg/10-g body weight for five consecutive days via intraperitoneal (i.p.) injection to 1-mo-old *FoxO1$^{f/f}$* and *FoxO1^{Agc1ER}* mice, 2-mo-old *Rosa-FoxO1$^{f/f}$* and *Rosa-FoxO1^{Agc1ER}* mice, and 2-wk-old *Col2Cre^{ERT2}*, *Col2Cre^{ERT2};Tgf-βr2$^{f/f}$*, *Col2Cre^{ERT2};Rosa-FoxO1$^{f/f}$*, and *Col2Cre^{ERT2};Tgf-βr2$^{f/f}$;Rosa-FoxO1$^{f/f}$* mice, respectively. Immediately following tamoxifen injection to *Rosa-FoxO1^{Agc1ER}* mice and their littermate controls, MLI was created unilaterally in the knee joints as previously described (41). Briefly, under general anesthesia with isoflurane, the mouse knee joint was first exposed by a medial capsular incision. The medial collateral ligament was transected under a dissection microscope using a microsurgical technique, and the 4-mm medial meniscus tissue was, subsequently, removed through the same procedure. After irrigation with saline to remove tissue debris, the medial capsular incision was sutured, and the skin incision was finally closed. Alternatively, tamoxifen was administrated to *Rosa-FoxO1^{Agc1ER}* and their control mice 1 wk after MLI surgery to examine any therapeutic effect of FoxO1 overexpression on injury-induced OA.

Histological Analyses. Mouse knee joints were collected at indicated time points and fixed in 10% neutral buffered formalin for 3 d. These specimens were decalcified for 3 d in formic acid decalcifier (ImmunoCal; StatLaboratory, no. 1414–1), processed and embedded in paraffin, and sectioned at a thickness of 5 μm. Sections were stained with safranin-O/fast green or picrosirius red to analyze phenotypical changes or collagen fiber alignment within the knee joints, respectively. Following staining, sections were scanned using NanoZoomer 2.0-HT whole slide imager (Hamamatsu), and cartilage thickness and cellularity above the tidemark in the cartilage of the tibial plateau were, subsequently, measured using NDP.View 2 software with the scanned images. Articular cartilage thickness was measured as the distance between the articular surface and the subchondral bone interface across three points in each medial tibial plateau of the knee joint in mice at 4 mo of age. Histological scoring of OA-like changes in the medial femoral condyle and tibial plateau were performed using the established OARSI scoring system (score, 0–6) (42). Three sections for each specimen were examined for all quantitative histomorphometric analyses. Immunohistochemistry staining for Prg4 (1:200; Abcam; no. ab28484), Col2A1 (1:100; ThermoFisher Scientific; no. MS235-P), Col10A1 (1:100; Quartet; no. 1-CO097-05), Mmp13 (1:200; Abcam; no. ab39012), PCNA (1:200; Abcam; no. ab92552), and LC3B (1:200; Novus Biologicals; no. NB100) were performed on paraffin sections following appropriate antigen retrieval methodologies. The signal was developed with DAB reagents (Vector Laboratories; no. SK-4100) and counterstained with hematoxylin or methyl green. To assess apoptosis, TUNEL staining was performed on paraffin sections with a in situ Cell Death Detection kit, Fluorescein (Roche; no. 11684795910) according to the manufacturer's instructions. Tissues prepared for frozen sections were fixed 4% paraformaldehyde for overnight, decalcified with 14% (ethylenedinitrilo)tetraacetic acid for 3 d, infiltrated with gradient sucrose for 2 d, embedded with tissue-TEK OCT medium, and sectioned at a thickness of 10 μm with a Leica CM1950 manual cryostat. Immunofluorescence staining for GFP (1:200; Abcam; no. ab13970) was performed on frozen knee sections. GFP fluorescence was imaged using Zeiss LSM 880 II Airscan Fast Confocal Microscope. Images of picrosirius red stained sections were obtained using a polarized microscope. Intensity of the picrosirius red stained area was measured by ImageJ software 1.52e.

Micro-CT Analyses. Micro-CT analyses were performed on 3-–5-, and 7-mo-old mouse knee joints prior to decalcification using a VivaCT 40 scanner. Briefly, the tibia was scanned from the knee to the connection at the fibula using a protocol consisting of high-resolution (10-μm) X-ray energy settings of 55 kVp and 145 μA and 300-ms integration time. Parameters of subchondral bone, including tissue volume, bone volume, bone mineral density, trabecular thickness, trabecular spacing, and trabecular number were measured as previously described using the Scanco analysis software (43). For the knee joints with MLI injuries, analyses were focused on the medial tibial plateau in order to reveal more apparent pathological changes.

Primary Articular Chondrocyte Cultures. Murine articular chondrocytes were isolated as described (44) with modifications. Briefly, articular cartilages were dissected from femoral heads and digested for 4–6 h in 0.5-mg/mL Collagenase P (Roche; no. 11249002001) in high-glucose Dulbecco's modified

Eagle's medium (DMEM) (Gibco; no. 31053028) supplemented with 1% penicillin/streptomycin. Following digestion, cells were harvested and seeded at a density of 50×10^4 cells/well, 25×10^4 cells/well, or 5×10^4 cells/well in 12-, 24-, or 96-well plates, respectively, according to experimental designs. The next day after plating, cells were treated with TGF-β1 (5 ng/mL) (R&D Systems; no. 240-B-002/CF) or vehicle for 24 h. In the experiments associated with inhibitors, cells were pretreated with Smad3 inhibitor SIS3 (Calbiochem; no. 566405) (45) or TAK1 inhibitor (5Z)-7-oxozeaenol (Tocris; no. 3604) (46) at a final concentration of 10 or 2.5 μM, respectively, or DMS as the control for 30 min, and then treated with TGF-β1 in the presence or absence of inhibitors for 24 h. In the FoxO1 LOF and GOF in vitro studies, primary articular chondrocytes isolated from *FoxO1*$^{f/f}$ or *Rosa-FoxO1*$^{f/f}$ mice were transduced with adenoviruses expressing GFP (Ad-Con) or Cre (Ad-Cre) at a multiplicity of 50 in the presence of polybrene (10 μg/mL) (Millipore; no. TR-1003-G) in high-glucose DMEM supplemented with 2% fetal bovine serum ([FBS]; Gibco; no. 10437) for 24 h. Following viral infection, cells were cultured in complete media (high-glucose DMEM supplemented with 10% FBS, 2-mM L-glutamine [Gibco; no. A2916801], and 1% penicillin/streptomycin) allowing cell recovery and gene expression. Forty-eight h later, cells were harvested for extraction of RNA or protein. For in vitro assessment of autophagic flux, cells were treated with bafilomycin (Sigma-Aldrich; no. B1793) for 4 h prior to protein extraction. For gene expression analyses regarding Rapa treatment, cells were incubated with 500-nM Rapa for the last 6 h before proceeding to RNA isolation.

Quantitative Gene Expression and Western Blot Analyses. RNA was isolated from primary articular chondrocytes using an RNeasy Mini kit (Qiagen; no. 74134). cDNA synthesis (iScript complementary DNA synthesis kit; Bio-Rad; no. 1708841) and real-time qPCR (SYBR master mix; Bio-Rad; no. 172–5274) were performed according to the manufacturers' instructions. Sequences of primers specific for *FoxO1*, *FoxO3*, *FoxO4*, *Agc1*, *Col2a1*, *Adamts5*, *Mmp13*, and β-*actin* are presented in *SI Appendix*, Table S3. Western blot analyses were conducted with protein lysates from primary articular chondrocytes. The following primary antibodies were used: p-Smad3 (1:1,000; Abcam; no. ab52903), Smad3 (1:1,000; Abcam; no. ab40854), p-P38 (1:500; Cell Signaling Technology; no. 9211S), P38 (1:1,000; Cell Signaling Technology; no. 9212S), FoxO1(1:1,000; Cell Signaling Technology; no. 2880S), FoxO3 (1:500; Cell Signaling Technology; no. 2497S), FoxO4 (1:500; Cell Signaling Technology; no. 9472T), LC3B (1:1,000; Novus Biologicals; no. NB100), and β-actin (1:4,000; Sigma-Aldrich, no. 2228).

ROS Detection and Cell Death Detection Assays. Primary articular chondrocytes were pretreated according to the experimental designs and, subsequently, incubated with Rapa (500 nM) or H_2O_2 (500 μM) for 2 or 1 h, respectively. Intracellular ROS levels were measured with a ROS detection kit according to the manufacturers' instructions (DCFDA Cellular ROS Detection Assay kit; Abcam; no. ab113851). For experiments to assess cell viability, cells were incubated with H_2O_2 (500 μM) for 24 h following virally induced FoxO1 overexpression. Cell death was determined using a Roche Cell Death Detection enzyme-linked immunosorbent assay kit (Roche; no. 11774425001). Cell viability was calculated as the percent absorbance of H_2O_2-treated cells compared to the H_2O_2-untreated cells.

ChIP Assays. ATDC5 cells (Sigma-Aldrich; no. 99072806) were maintained in DMEM/F12 (1:1) medium (Gibco; no. 11320033) supplemented with 5% FBS. Upon ChIP experiments, 1×10^7 cells were harvested. Briefly, cells were fixed with formaldehyde and chromatin was sheared to 200–500 bp using Bioruptor Pico (Diagenode). After confirmation of successful sonication, sheared chromatin (equivalent to 3×10^6 cell per i.p.) was immunoprecipitated with a ChIP grade anti-FoxO1A antibody (3 μg per i.p.; Abcam; no. ab39670), while anti-histone H3 antibody (1 μg per i.p.; Abcam; no. ab12079) and Rabbit IgG (1 μg per i.p.; Abcam; no. ab171870) were used as positive and negative controls, respectively. Following reverse cross-linking of protein–DNA, the enrichment of DNA fragments during immunoprecipitation was analyzed by standard PCR and real-time qPCR. Primer sequences for ChIP-PCR are listed in *SI Appendix*, Table S3.

LC3 Promoter Luciferase Assays. Software search for FoxO1 binding sites using LASAGNA-Search 2.0 (47) identified multiple putative sites in the promoter regions of the *Maplc3b* gene. The *Mapl3b* promoter region corresponding to a mouse genomic DNA fragment (–1608 to –1379), which contains the FoxO1 consensus binding sequence nearest the transcription start site, was selected for subcloning. This native DNA fragment and the Mut version in the FoxO1 binding sites (TTGTTTGC → TGGGCGGC) were synthesized by GenScript and subcloned into the pGL4.10[Luc2] vector (Promega; no. E6651) to generate two constructs. These constructs, including basic promoterless vector pGL4.10[Luc2], LC3-Luc2, and mutLC3-Luc2, were transfected into virally induced FoxO1 overexpression articular chondrocytes with lipofectamine 2000 transfection reagents (ThermoFisher Scientific; no. 11668027). Luciferase assays were performed 48 h following transfection using a Luciferase Assay System (Promega; no. E1500).

Statistical Analyses. All data were expressed as means ± SD. Results were analyzed GraphPad Prism version 7 (GraphPad Software, Inc.). Comparisons between two groups were analyzed using two-tailed unpaired Student's *t* test. One-way ANOVA was used when comparing multiple groups, followed by a Bonferroni test as appropriate for subsequent pairwise (group) comparisons. A *P* value less than 0.05 was considered statistically significant.

Data Availability. All study data are included in the article and *SI Appendix*.

ACKNOWLEDGMENTS. We thank Dr. Benoit de Crombrugghe and Dr. Herbert Virgin for providing important mouse strains. We would like to gratefully acknowledge the technical expertise and assistance of Daniel Leib and Michael Brodt from Structure and Strength Core, and Crystal Idleburg and Samantha Coleman from Musculoskeletal Histology and Morphometry Core within the Musculoskeletal Research Center. This paper was supported by the following NIH Grants: R01 grants (AR075860 and AR077616 to J.S. as well as AR069605 to R.J.O.), a R21 grant (AR077226 to J.S.), a T32 training grant that supported C.W. (AR060719), and a P30 Core Center Grant (AR057235).

1. D. T. Felson, Clinical practice. Osteoarthritis of the knee. *N. Engl. J. Med.* **354**, 841–848 (2006).
2. J. Shen, Y. Abu-Amer, R. J. O'Keefe, A. McAlinden, Inflammation and epigenetic regulation in osteoarthritis. *Connect. Tissue Res.* **58**, 49–63 (2017).
3. M. Wang *et al.*, Recent progress in understanding molecular mechanisms of cartilage degeneration during osteoarthritis. *Ann. N. Y. Acad. Sci.* **1240**, 61–69 (2011).
4. J. W. Bijlsma, F. Berenbaum, F. P. Lafeber, Osteoarthritis: An update with relevance for clinical practice. *Lancet* **377**, 2115–2126 (2011).
5. J. Martel-Pelletier *et al.*, Osteoarthritis. *Nat. Rev. Dis. Primers* **2**, 16072 (2016).
6. M. B. Mueller, R. S. Tuan, Anabolic/catabolic balance in pathogenesis of osteoarthritis: Identifying molecular targets. *PMR* **3** (suppl. 1), S3–S11 (2011).
7. J. Shen *et al.*, Deletion of the transforming growth factor β receptor type II gene in articular chondrocytes leads to a progressive osteoarthritis-like phenotype in mice. *Arthritis Rheum.* **65**, 3107–3119 (2013).
8. R. Serra *et al.*, Expression of a truncated, kinase-defective TGF-beta type II receptor in mouse skeletal tissue promotes terminal chondrocyte differentiation and osteoarthritis. *J. Cell Biol.* **139**, 541–552 (1997).
9. X. Yang *et al.*, TGF-beta/Smad3 signals repress chondrocyte hypertrophic differentiation and are required for maintaining articular cartilage. *J. Cell Biol.* **153**, 35–46 (2001).
10. L. Gao *et al.*, TAK1 regulates SOX9 expression in chondrocytes and is essential for postnatal development of the growth plate and articular cartilages. *J. Cell Sci.* **126**, 5704–5713 (2013).
11. S. Namdari, L. Wei, D. Moore, Q. Chen, Reduced limb length and worsened osteoarthritis in adult mice after genetic inhibition of p38 MAP kinase activity in cartilage. *Arthritis Rheum.* **58**, 3520–3529 (2008).
12. I. Prasadam *et al.*, Inhibition of p38 pathway leads to OA-like changes in a rat animal model. *Rheumatology (Oxford)* **51**, 813–823 (2012).
13. A. J. Kahn, FOXO3 and related transcription factors in development, aging, and exceptional longevity. *J. Gerontol. A Biol. Sci. Med. Sci.* **70**, 421–425 (2015).
14. Y. Wang, Y. Zhou, D. T. Graves, FOXO transcription factors: Their clinical significance and regulation. *BioMed Res. Int.* **2014**, 925350 (2014).
15. J. H. Paik *et al.*, FoxOs are lineage-restricted redundant tumor suppressors and regulate endothelial cell homeostasis. *Cell* **128**, 309–323 (2007).
16. F. M. Jacobs *et al.*, FoxO6, a novel member of the FoxO class of transcription factors with distinct shuttling dynamics. *J. Biol. Chem.* **278**, 35959–35967 (2003).
17. A. Eijkelenboom, B. M. Burgering, FOXOs: Signalling integrators for homeostasis maintenance. *Nat. Rev. Mol. Cell Biol.* **14**, 83–97 (2013).
18. L. Partridge, J. C. Brüning, Forkhead transcription factors and ageing. *Oncogene* **27**, 2351–2363 (2008).
19. M. T. Rached *et al.*, FoxO1 is a positive regulator of bone formation by favoring protein synthesis and resistance to oxidative stress in osteoblasts. *Cell Metab.* **11**, 147–160 (2010).
20. M. Sandri *et al.*, Foxo transcription factors induce the atrophy-related ubiquitin ligase atrogin-1 and cause skeletal muscle atrophy. *Cell* **117**, 399–412 (2004).
21. Y. Akasaki *et al.*, Dysregulated FOXO transcription factors in articular cartilage in aging and osteoarthritis. *Osteoarthritis Cartilage* **22**, 162–170 (2014).
22. T. Matsuzaki *et al.*, FoxO transcription factors modulate autophagy and proteoglycan 4 in cartilage homeostasis and osteoarthritis. *Sci. Transl. Med.* **10**, eaan0746 (2018).
23. G. Eelen *et al.*, Forkhead box O transcription factors in chondrocytes regulate endochondral bone formation. *J. Steroid Biochem. Mol. Biol.* **164**, 337–343 (2016).

24. C. Buckland-Wright, Subchondral bone changes in hand and knee osteoarthritis detected by radiography. *Osteoarthritis Cartilage* **12**, 10–19 (2004).
25. N. Furuya, J. Yu, M. Byfield, S. Pattingre, B. Levine, The evolutionarily conserved domain of Beclin 1 is required for Vps34 binding, autophagy and tumor suppressor function. *Autophagy* **1**, 46–52 (2005).
26. Y. Ohsumi, N. Mizushima, Two ubiquitin-like conjugation systems essential for autophagy. *Semin. Cell Dev. Biol.* **15**, 231–236 (2004).
27. C. López-Otín, M. A. Blasco, L. Partridge, M. Serrano, G. Kroemer, The hallmarks of aging. *Cell* **153**, 1194–1217 (2013).
28. Q. Peng *et al*., Autophagy maintains the stemness of ovarian cancer stem cells by FOXA2. *J. Exp. Clin. Cancer Res.* **36**, 171 (2017).
29. R. Vivar *et al*., FoxO1 mediates TGF-beta1-dependent cardiac myofibroblast differentiation. *Biochim. Biophys. Acta* **1863**, 128–138 (2016).
30. T. S. Buttrick *et al*., Foxo1 promotes Th9 cell differentiation and airway allergy. *Sci. Rep.* **8**, 818 (2018).
31. R. R. Gomis *et al*., A FoxO-Smad synexpression group in human keratinocytes. *Proc. Natl. Acad. Sci. U.S.A.* **103**, 12747–12752 (2006).
32. B. Caramés, N. Taniguchi, S. Otsuki, F. J. Blanco, M. Lotz, Autophagy is a protective mechanism in normal cartilage, and its aging-related loss is linked with cell death and osteoarthritis. *Arthritis Rheum.* **62**, 791–801 (2010).
33. N. T. Cheng *et al*., Role of autophagy in the progression of osteoarthritis: The autophagy inhibitor, 3-methyladenine, aggravates the severity of experimental osteoarthritis. *Int. J. Mol. Med.* **39**, 1224–1232 (2017).
34. B. Caramés *et al*., Autophagy activation by rapamycin reduces severity of experimental osteoarthritis. *Ann. Rheum. Dis.* **71**, 575–581 (2012).
35. N. Mizushima, A. Yamamoto, M. Matsui, T. Yoshimori, Y. Ohsumi, In vivo analysis of autophagy in response to nutrient starvation using transgenic mice expressing a fluorescent autophagosome marker. *Mol. Biol. Cell* **15**, 1101–1111 (2004).
36. A. Brunet *et al*., Stress-dependent regulation of FOXO transcription factors by the SIRT1 deacetylase. *Science* **303**, 2011–2015 (2004).
37. L. O. Klotz *et al*., Redox regulation of FoxO transcription factors. *Redox Biol.* **6**, 51–72 (2015).
38. S. Iyer *et al*., FOXOs attenuate bone formation by suppressing Wnt signaling. *J. Clin. Invest.* **123**, 3409–3419 (2013).
39. F. Xu *et al*., Disruption of a mitochondrial RNA-binding protein gene results in decreased cytochrome b expression and a marked reduction in ubiquinol-cytochrome c reductase activity in mouse heart mitochondria. *Biochem. J.* **416**, 15–26 (2008).
40. S. P. Henry *et al*., Generation of aggrecan-CreERT2 knockin mice for inducible Cre activity in adult cartilage. *Genesis* **47**, 805–814 (2009).
41. S. Kamekura *et al*., Osteoarthritis development in novel experimental mouse models induced by knee joint instability. *Osteoarthritis Cartilage* **13**, 632–641 (2005).
42. S. S. Glasson, M. G. Chambers, W. B. Van Den Berg, C. B. Little, The OARSI histopathology initiative - recommendations for histological assessments of osteoarthritis in the mouse. *Osteoarthritis Cartilage* **18** (suppl. 3), S17–S23 (2010).
43. E. R. Sampson *et al*., Establishment of an index with increased sensitivity for assessing murine arthritis. *J. Orthop. Res.* **29**, 1145–1151 (2011).
44. M. Gosset, F. Berenbaum, S. Thirion, C. Jacques, Primary culture and phenotyping of murine chondrocytes. *Nat. Protoc.* **3**, 1253–1260 (2008).
45. M. Jinnin, H. Ihn, K. Tamaki, Characterization of SIS3, a novel specific inhibitor of Smad3, and its effect on transforming growth factor-beta1-induced extracellular matrix expression. *Mol. Pharmacol.* **69**, 597–607 (2006).
46. J. Wu *et al*., Mechanism and in vitro pharmacology of TAK1 inhibition by (5Z)-7-Oxozeaenol. *ACS Chem. Biol.* **8**, 643–650 (2013).
47. C. Lee, C. H. Huang, LASAGNA-search 2.0: Integrated transcription factor binding site search and visualization in a browser. *Bioinformatics* **30**, 1923–1925 (2014).